http://dx.doi.org/10.5012/bkcs.2012.33.1.209

# Preparation and Characterization of Reduced Graphene Nanosheets *via* Pre-exfoliation of Graphite Flakes

**Long-Yue Meng and Soo-Jin Park***

*Department of Chemistry, Inha University, Incheon 402-751, South Korea. *E-mail: sjpark@inha.ac.kr*
*Received July 18, 2011, Accepted November 21, 2011*

In this work, the reduced graphene nanosheets were synthesized from pre-exfoliated graphite flakes. The pristine graphite flakes were firstly pre-exfoliated to graphite nanoplatelets in the presence of acetic acid. The obtained graphite nanoplatelets were treated by Hummer's method to produce graphite oxide sheets and were finally exfoliated to graphene nanosheets by ultrasonication and reduction processes. The prepared graphene nanosheets were studied by X-ray photoelectron spectroscopy (XPS), X-ray diffraction (XRD), atomic force microscopy (AFM), and transmission electron microscopy (TEM). From the results, it was found that the pre-exfoliation process showed significant influence on preparation of graphite oxide sheets and graphene nanosheets. The prepared graphene nanosheets were applied to the preparation of conductive materials, which yielded a greatly improved electrical resistance of 200 Ω/sq.

**Key Words :** Graphene nanosheets, Acetic acid, Pre-exfoliation

## Introduction

Graphene is an atomic scale honeycomb lattice made of carbon atoms. Recently, the isolation of a single layer of graphene from graphite has attracted increasing attention because the resulting graphene exhibits novel physico-chemical properties such as high values of its Yong's modulus, fracture strength, thermal conductivity, specific surface area, and electrical conductivity.[1] Therefore, graphene nanaosheets have attracted considerable interest due to their peculiar properties in fundamental research and potential industrial applications in energy storage materials, polymer composites, and transparent conductors.[2-6]

Direct synthesis of the graphene had not been possible, although the materials had been conceptually conceived and theoretically predicted to be capable of exhibiting many novel and useful properties. Since Novoselov *et al.* in 2004 found a way to isolate individual graphene planes by using scotch tape,[1] many researchers have attempted to create large scale graphene using physico-chemical methods such as epitaxial growth on silicon carbide or a metal substrate.[7,8] However, such synthesis methods have revealed lower yields and certain unexpected properties.

Graphene can be obtained from the cleavage of natural graphite, which consists of a stack of flat graphene sheets. Graphene, due to their high specific surface area, tend to form irreversible bulk or even restack to form graphite through van der Waals interactions.[4] Up to now, graphene are usually prepared by chemical processing, including graphite oxidation, exfoliation, and reduction. This method is the most suitable for the large-scale production of single graphene at low cost.[9] Chemical oxidation of graphite followed by subsequent exfoliation intercalates graphite with an expandable intercalation agent (such as sulfuric acid and nitric acid) to form a graphite intercalation compound.[10,11] However, the graphite oxide prepared by the traditional chemical oxidation method is incomplete. Increasing the effective surface area and surface acidic functional groups of graphite for reaction is an option to improve the oxidation efficiency. The pristine graphite is difficult to exfoliate into graphite plates unless they are treated by appropriate molecules. Geng *et al.* fully pre-exfoliated pristine graphite to graphite nanopalates by ultrasonication in the presence of formic acid.[12] Pre-exfoliation with formic acid improved the efficiency and speed of the preparation of graphene compared to currently used techniques.

In this work, we pre-exfoliated graphite flakes with acetic acid instead of formic acid to obtain graphite nanoplatelets. The obtained graphite nanoplatelets were treated by Hummer's method to produce graphite oxide sheets and, finally, exfoliated to graphene nanosheets by ultrasonication and reduction processes. The prepared graphene nanosheets were studied by X-ray photoelectron spectroscopy (XPS), X-ray diffraction (XRD), atomic force microscopy (AFM), and transmission electron microscopy (TEM). The prepared graphene nanosheets films are applied to the preparation of conductive materials.

## Materials and Methods

**Preparation of Graphene Nanosheets.** (a) A sample of 1.0 g of pristine graphite flakes was immersed in 50 mL of formic acid, and then ultrasonicated for 2 h at room temperature.[10] (b) A sample of 1.0 g of pristine graphite flakes and 50 mL of acetic acid was mixed by ultrasonication method for 2 h, and then stay for one week. These resulting graphite nanoplatelets were washed with acetone, and then dried in an oven at 80 °C for 12 h. The sample was designated as GP. (c) Another 1.0 g of pristine graphite flakes was treated with 50 mL of $HNO_3/H_2SO_4$ (the volume

ratio of 1:3) mixture solutions by ultrasonication method for 2 h, and then thermal treatment at 800 °C for 120 s.[11]

Above prepared graphite nanoplatelets were carried out based on Hummer's method.[7] 1.0 g of pre-treated graphite nanoplatelets and 0.5 g $NaNO_3$ were added into 23 mL of concentrated $H_2SO_4$ at 0 °C. With vigorous stirring, 3 g of $KMnO_4$ was gradually added, and the temperature of the mixture was controlled under 20 °C. The ice bath was then removed, and the temperature of the mixture was maintained at 35 °C for 0.5 h. Then, 46 mL $H_2O$ was added into the mixture slowly, which made the mixture boil. After 15 min, 140 mL of hot water and $H_2O_2$ aqueous solution were added into the deeply brown mixture with stirring. The resulting suspension was filtered while it was still hot. The solid mixture was washed with 5% HCl aqueous solution and acetone, respectively. The resulting solid was dried at 60 °C under vacuum. The obtained graphite oxide was designated as GO-F (a), GO-A (b), and GO-E (c), respectively. The prepared graphene oxide was designated as GO by traditional method. Finally, 0.1 g graphite oxide was dispersed in 100 mL $H_2O$ *via* ultrasonication and then $NaBH_4$ was added to reduce the graphene oxide nanosheets to graphene nanosheets at 80 °C. The prepared graphene nanosheets was designated as GN-F (a), GN-A (b), GN-E (c), and GN (traditional method), respectively.

**Characterization.** X-ray photoelectron spectroscopy (XPS) measurements were performed on an ESCALAB220i-XL (VG Scientific) spectrometer with monochromatized Mg Kα X-ray radiation as the X-ray source for excitation in order to confirm the surface chemistry of graphite flakes and graphite oxide. To identify the types and percentages of the functional groups on the surface of the obtained graphite oxide, the C1s peaks of the XPS pattern were curve-fitted. Corresponding images of the graphene nanosheets were obtained by atomic force microscopy (AFM, Nanoscope Multimode IV a/Digital Instrument), scanning electron microscope (SEM, Hitach S-4200), and transmission electron microscopy (TEM, JEM2100F/JEOL). The structural properties of the samples were also evaluated through an X-ray diffractometer (XRD, DMAX 2500/Rigaku) with Cu Kα radiation. The electrical resistivity of samples was measured by a four-probe tester (Mitsubishi, MCP-T610).

## Results and Discussion

**Surface Chemistry.** XPS is used to investigate the introduction of atomic concentrations on the pristine graphite flakes, graphite nanoplatelets, graphite oxide sheets, and graphene nanosheets, as shown in Figure 1. From the figure, the XPS spectrum of the samples shows carbon peaks (285.1 eV) and oxygen peaks (533.4 eV). The oxygen concentration of pristine graphite flakes was only a small proportion of 0.87%, but after chemical oxidation treatment, it drastically increased to 30.79% (see Table 1). The results showed that the chemical oxidation step introduced a large amount of oxygen functional groups on the graphite surface. Table 1 also shows that the oxygen peak of graphite nanoplatelets (GP) is stronger than the pristine graphite flakes. The natural graphite flakes were oxidized and directly exfoliated by ulrtasonication in acetic acid. This is probably due to that the existence of amounts of hydroxyl, carboxyl, carbonyl, and epoxide functional groups attached onto the basal or edge plane.[12] Moreover, the graphite oxide pretreated with acetate acid solution showed the highest O/C ratio. Increased oxygen contents may be formed from epoxide, hydroxyl, carbonyl, and carboxyl groups, which broke the carbon sigma bonds and transformed them into single C-C or $sp^3$ bonds.[12-14]

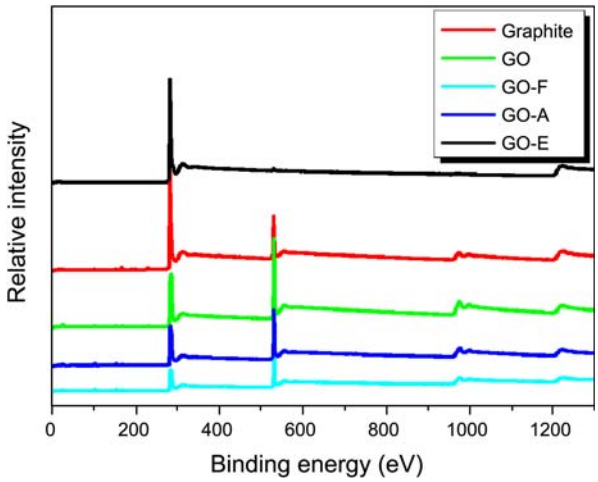


**Figure 1.** XPS general spectra of graphite flakes and graphite oxide sheets before and after the different pre-treatments.

**Table 1.** Atomic concentrations of graphite flakes, graphite nanoplatelets (GP), chemical oxidized graphite oxide before and after the different pre-treatment, and graphene nanosheets (GN-A)

| Samples | Elements (%) | | |
|---|---|---|---|
| | C 1s | O1s | O/C ratio |
| Graphite | 99.13 | 0.87 | 0.009 |
| GP | 91.73 | 8.27 | 0.091 |
| GO | 81.98 | 15.65 | 0.191 |
| GO-F | 69.49 | 29.52 | 0.425 |
| GO-A | 65.94 | 30.79 | 0.467 |
| GO-E | 70.86 | 26.52 | 0.374 |
| GN-A | 93.19 | 6.81 | 0.073 |

XPS is also a valuable tool used in the detection of the different oxygen-containing functional groups that form on the carbon surface during the chemical oxidation process. Figure 2 presents the typical C1s spectra of the sample surface studied here. The C1s signal shows that the deconvolution of the C1s spectra yields four peaks with different binding energy values representing carbon in the non-oxygenated C–C or C–H (284.5 eV), single C–O bonds (285.5 eV), double C=O bonds (carbonyl, 287.1 eV), and carboxylic COOH or O–C=O (288.5 eV).[15] The relative concentrations of surface functional groups obtained from the deconvolution of the C1s XPS regions are summarized in Table 2, which shows that the non-oxygenated C–C or

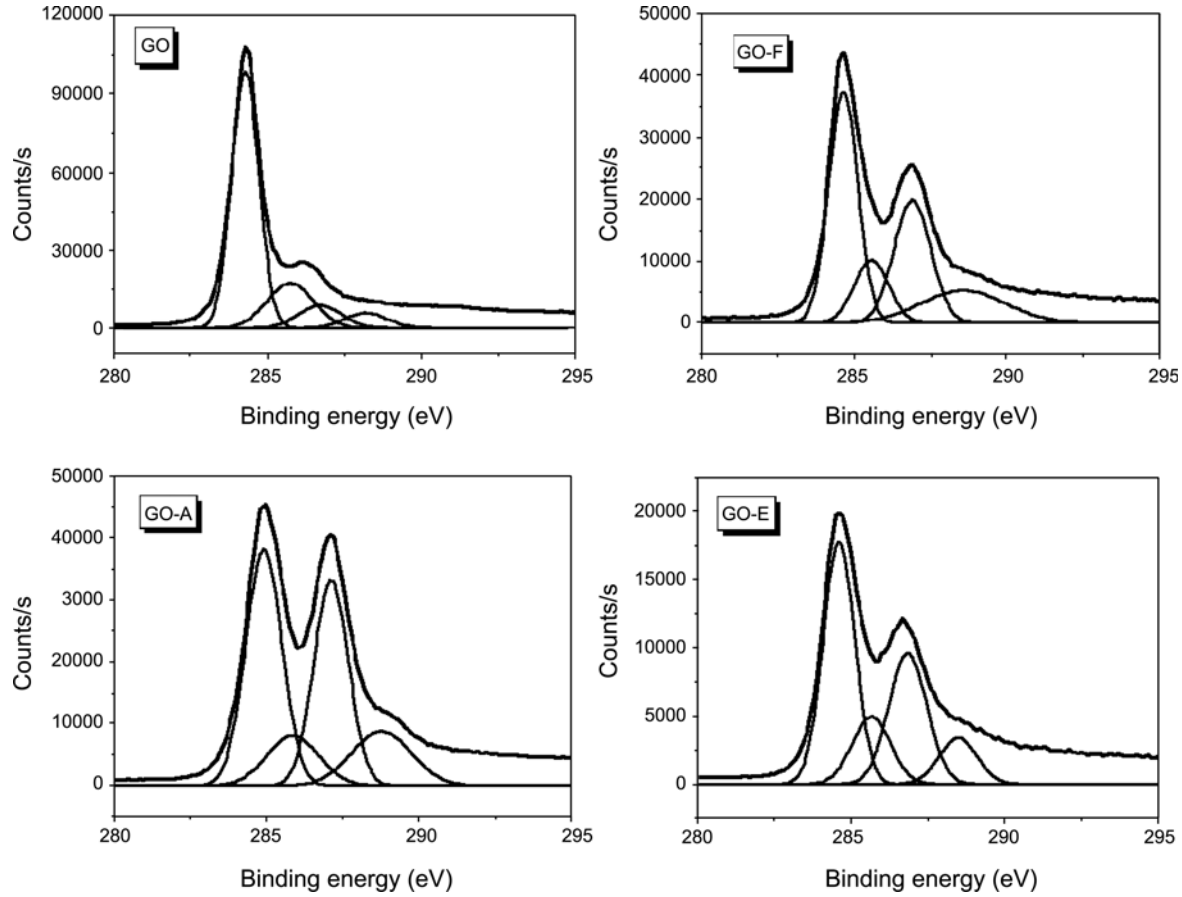


**Figure 2.** $C_{1s}$ XPS spectra and deconvolution of the graphite oxide sheets before and after the different pre-treatment.

C–H groups of the prepared GO-A are much fewer than those of the GP. The main peak changes in the GO-A compared with the peaks of the GO at 285.5 eV, 287.1 eV, and 288.5 eV, which vary greatly in intensity.

Allowing for the results obtained for GO-A, it follows that the chemical oxidation treatments of GP yields different surface oxygen functional groups such as C-O, C=O, and COOH. In addition, the formation of oxygen functional groups of GO-A oxygen functional groups of GO-A is significantly larger than GO. According to the pertinent literature, the formation of C-O groups after the oxidation of the epoxide (1,2-ether oxygen) are located on the aromatic carbon atoms, and the hydroxyl groups are distributed randomly throughout the carbon basal plane. The carboxyl groups are likely located at the edges of the graphite oxide sheets.[16] The results showed that the acetate acid pre-exfoliation introduced a greater amount of acidic oxygen groups such as C=O and O-C=O compared with GO.

Table 1 also shows that the reduction step decreased much of the oxygen content on the surface of GO-A, reducing the O/C ratio from 0.467 to 0.073. The C1s signal of GN shows a much smaller contribution of the oxygenated carbons, indicating that deoxygenation has occurred at the carbon surface. As shown in Table 2, the distribution of C-O bonds of GN-A is decreased to 8.4%, which is probably due to the reduction of oxygen functional groups of graphene oxide by

**Table 2.** Surface group distributions obtained from deconvolution of $C_{1s}$ XPS regions of the graphite oxide (before and after the different pre-treatment) and graphene nanosheets (GN-A)

| $C_{1s}$ | Assessment | Surface group distributions (%) | | | | |
|---|---|---|---|---|---|---|
| | | GO | GO-F | GO-A | GO-E | GN-A |
| 284.5 | C-C; C-H | 81.7 | 41.6 | 39.8 | 45.1 | 72.4 |
| 285.8 | C-O-C | 10.3 | 13.4 | 12.0 | 15.2 | 8.4 |
| 287.1 | C=O | 4.8 | 27.9 | 33.1 | 29.3 | 9.1 |
| 288.5 | COOH; O–C=O | 3.2 | 17.1 | 15.1 | 10.3 | 10.1 |

$NaBH_4$.[17,18] However, the C1s signal of the reduced graphene oxide also shows some of these oxygen functional groups due to the incomplete reduction. This indicates that the reduction of the $NaBH_4$ yields a deoxygenated $sp^2$ carbon from the epoxides and hydroxyls.

**Structural Properties.** The structural properties of pristine graphite flakes, graphite oxide sheets, and graphene nanosheets were characterized using the XRD analysis, as shown in Figure 3. For the pristine graphite flakes, the sharp and intensive peaks at $2\theta=26.6^{o}$ and $2\theta=24.4^{o}$ indicated the highly organized layered structure with interlayer spacing of 0.330 and 0.365 nm (Fig. 3(a)). After acetic acid pre-exfoliation, the interlayer spacing of graphite flakes is increased from 0.330 to 0.336 nm. However, the degree of exfoliation of graphite nanoplatelets is too small, which is due to

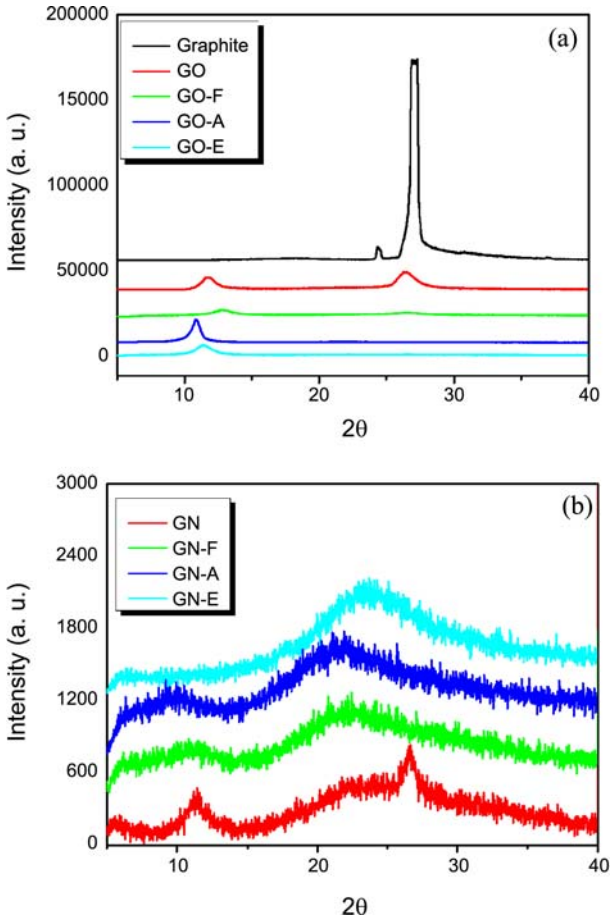


**Figure 3.** XRD patterns of the graphite (a), graphite nanoplatelets (a), graphite oxide sheets (a), and the reduced graphene nanosheets before and after the different pre-treatments (b).

the acetic acid is a week oxidant and the ultrasonicator exfoliates the graphite flakes to smaller particles.

Previous research reported that the inter-layers of graphite can be intercalated by various molecular or ions.[19,20] In addition, the XPS data of GP shows that oxygen functional groups are introduced into the surface of graphite (Table 1). Therefore, the increased interlayer spacing is due to the formation of oxygen groups on the surface of graphene and exfoliation of graphite nanoplatelets with a thickness in-nanometer scale for complete oxidation efficiency by avoid graphite core/graphite oxide shell particles.

As the other previous research reported, the step of pre-oxidation is an option to improve the oxidation efficiency for increasing the effective surface area of graphite for reaction before the Hummers method. In our experiment, we used a mixture of $KMNO_4$, $HNO_3$, and $H_2SO_4$ to chemically oxidize the pristine graphite flakes by the Hummer's method. During the chemical oxidation process, oxygen functional groups, $NO_3^-$, and $SO_4^{2-}$ can insert themselves into the graphene layers.[21,22] As shown in Figure 3(a), after chemically oxidition, the XRD patterns of GO-A correspond to a layered structure with a basal spacing of 0.820 nm. As can be seen, the XRD patterns of graphite oxide sheets show a typical broad peak with an obvious disappearance of the characteristic peaks, which might be attributed to very thin graphene layers due to high degree of exfoliation. This result indicated that the graphene nanosheets are exfoliated into a monolayer or a few-layer and obtained a new lattice structure, which is significantly different from the pristine graphite flakes and graphite oxide sheets.

We also determine the influence of pre-exfoliation of the graphite flakes by different pre-treatment methods on the structural of graphene nanosheets compared with the traditional method, as shown in Figure 3(b). The diffraction peak in the XRD pattern of GO-A appeared to be 10.8°, corresponding to the layer-to-layer distance of 0.820 nm, which is significantly larger than that of other graphite oxide sheets (GO: 0.749 nm, GO-F: 0.694 nm, and GO-E: 0.775 nm). It is due to the highest intercalating oxide functional groups of GO-A. As shown in Figure 3(b), whereas the XRD patterns of graphene nanosheets show a typical broad peak with an obvious disappearance of the characteristic peaks, which might be attributed to very thin graphene layers due to high degree of exfoliation. This result indicated that the graphene nanosheets were exfoliated into a monolayer or few-layers, resulting a new lattice structure, which is significantly different from the pristine graphie flakes and graphite oxide.

In the case of GN, the interlayer spacing of graphene nanosheets (2θ=26.7°, 0.335 nm) is smaller than other prepared graphene nanosheets (GN-E: 0.376 nm, GN-F: 0.415 nm, and GN-A: 0.400 nm). The higher basal spacing of GN-A may be due to the presence of residual oxygen and hydrogen, indicating incomplete reduction of graphite oxide sheets to graphene nanosheets. This result determined that the pre-exfoliation of graphite flakes led to the difference of graphene nanosheets in the interlayer spacing by intercalating oxide functional groups contents.

**Surface Morphologies.** The morphology of the prepared graphite nanoplatelets were studied using SEM and TEM. As shown in Figure 4, the particle size of graphite flakes and graphite nanoplatelets present distinct differences. Typical SEM images of the graphite flakes and graphite nanoplatelets are shown in Figure 4(a, b). Figure 4(a) shows the graphite flakes with the particle size in the range of 300-

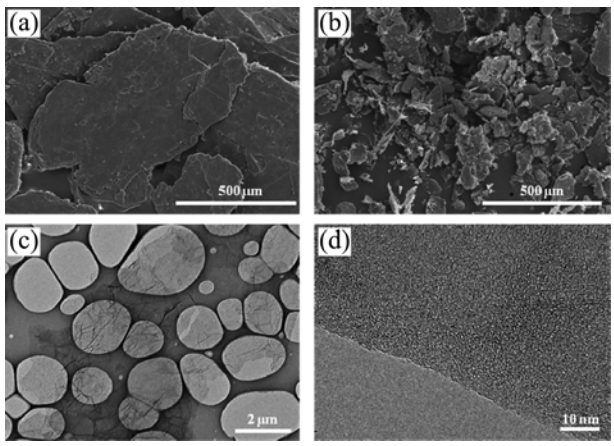


**Figure 4.** SEM (a, b) and TEM (c, d) images of graphite flakes (a), graphite nanoplatelets (b), and graphene nanosheets (GN-A, c-d).

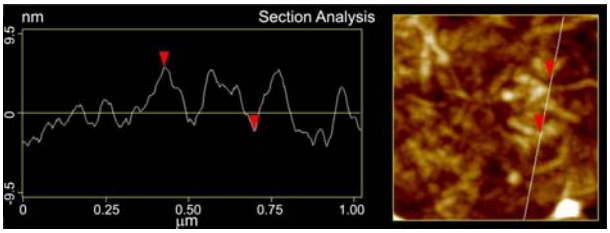


**Figure 5.** AFM topography images of graphene nanosheets (GN-A).

1000 μm. After acetic acid oxidation and ultrasonication for 2 h, the morphology of graphite flakes is strongly modified as well as the particle size, as shown on Figure 4(b). The exfoliated graphite nanoplatelets show smaller particles with the particle size in the range of 10-500 μm (Fig. 4b). Figure 4(c, d) shows that GN-A film is transparent and that the graphene consists of one-layers.[24] The interlayer spacing is measured to be 0.410 nm, which is consistent with the experimental value of 0.415 nm obtained from the above XRD results. AFM is also used to determine the thickness of the graphene-based sheets. As shown in Figure 5, graphenen nanosheets were deposited on the glass substrate. As can be seen, the fully exfoliated graphene are observed with an average nanosheets size of 250 nm. By line scanning across the plain area of nanosheets, the thickness of the graphene nanosheets obtained by acetate acid solution pre-exfoliation is about 4.5 nm. This value is still somewhat larger than the theoretical thickness for a perfectly flat $sp^2$-carbon-atom network.[23]

**Electrical Properties.** Recently, graphene based carbon materials are used as transparent and conductive materials.[15,25,26] The electrical conductivities of graphite oxide sheets and graphene nanosheets are evaluated at room temperature based on the four probe method, as shown in Table 3. The measured sheet resistance of GO-A and GN-A show a significant change. After chemical oxidation, the prepared GO-A exhibited a higher sheet resistance of 1850 Ω/sq. Pasricha *et al.* reported that the GO conducts electricity poorly, as it lacks an extended π-conjugated orbital system.[26] After the formation of GN-A, the sheet resistance of graphene nanosheets are decreased approximately 10 fold as compared to GO-A. The prominent recovery of sheet resistance to 200 Ω/sq of GN-A is due to the deoxygenation of GO-A to create C-C and C=C bonds, which has proven to be efficient in restoring the majority of $sp^2$ conjugated network, which are also reflected from the XPS result. Lee *et al.* prepared few-layer graphene sheets with a sheet resistance of 233 Ω/sq by CVD method.[27] The advantage of the average inter-sheet distances in GN-A leading to the lower sheet resistance of GN-A as compared to that of Lee's result. According to the results above, the increase in conductivity is an effect of reducing the average intersheet distances.[28-30]

**Table 3.** The sheet resistance of graphene oxide nanosheets (GO-A) and graphene nanaosheets (GN-A)

| Samples | Sheet resistance (Ω/sq) |
|---|---|
| GO-A | 1850 |
| GN-A | 200 |

## Conclusions

In conclusion, we successfully prepared reduced graphene nanosheets from the graphite nanoplatelets by chemical oxidation method and examined the effect of pre-exfoliation in the presence of acetic acid on exfoliation of graphite flakes. From the results, it was found that the pre-exfoliation process showed significant influence on preparation of graphite oxide sheets and graphene nanosheets. The interlayer spacing was larger than that of traditional method for the preparation of graphite oxide sheets, which was due to the more oxygenated functional groups graft on the graphite surfaces. In addition, the acetate acid pre-exfoliation greatly improved the efficiency in preparing stable graphene nanosheets, and showed a sheet resistance of 200 Ω/sq.

**Acknowledgments.** This research was supported by the Korea Ministry of Environment as the Eco-Innovation Project. Also, this work was supported by the Carbon Valley Project of the Ministry of Knowledge Economy, Korea.

## References

1. Novoselov, K. S.; Geim, A. K.; Morozov, S. V.; Jiang, D.; Zhang, Y.; Dubonos, S. V.; GrigorieVa, I. V.; Firsov, A. A. *Science* **2004**, *306*, 666.
2. Ghosh, A.; Subrahmanyam, K. S.; Krishna, K. S.; Datta, S.; Govindaraj, A.; Pati, S. K.; Rao, C. N. R. J. *Phys. Chem. B* **2008**, *112*, 15704.
3. Bai, H.; Li, C.; Wang, X.; Shi, G. *Chem. Comm.* **2010**, *46*, 2376.
4. Cai, D.; Song, M.; Xu, C. *Adv. Mater.* **2008**, *20*, 1706.
5. Ahn, K. S.; Seo, S. W.; Park, J. H.; Min, B. K.; Jung, W. S. *Bull. Korean. Chem. Soc.* **2011**, *32*, 1579.
6. Kim, B. J.; Byun, J. H.; Park, S. J. *Bull. Korean. Chem. Soc.* **2010**, *31*, 2261.
7. Sutter, P. *Nature Mater.* **2009**, *8*, 171.
8. Chae, S. J.; Günes, F.; Kim, K. K.; Kim, E. S.; Han, G. H.; Kim, S. M.; Shin, H. J.; Yoon, S. M.; Choi, J. Y.; Park, M. H.; Yang, C. W.; Pribat, D.; Lee, Y. H. *Adv. Mater.* **2008**, *21*, 2328.
9. Hummers, W. S.; Offeman, R. E. *J. Am. Chem. Soc.* **2008**, *8*, 3137.
10. Loh, K. P.; Bao, Q.; Ang, P. K.; Yang, J. *J. Mater. Chem.* **2010**, *20*, 2277.
11. Jang, B. Z.; Zhamu, A. *J. Mater. Sci.* **2008**, *43*, 5092.
12. Geng, Y.; Wang, S. J.; Kim, J. K. *J. Colloid Interface Sci.* **2009**, *336*, 592.
13. Kim, K. S.; Rhee, K. Y.; Lee, K. H.; Byund, J. H.; Park, S. J. *J. Ind. Eng. Chem.* **2010**, *16*, 572.
14. Schniepp, H. C.; Li, J. L.; McAllister, M. J.; Sai, H.; Herrera-Alonso, M.; Adamson, D. H.; Prud'homme, R. K.; Car, R.; Saville, D. A.; Aksay, I. A. *J. Phys. Chem. B* **2006**, *110*, 8535.
15. Becerril, H. A.; Mao, J.; Liu, Z.; Stoltenberg, R. M.; Bao, Z.; Chen, Y. *ACS Nano* **2008**, *2*, 463.
16. Yang, D.; Velamakanni, A.; Bozoklu, G.; Park, S.; Stoller, M.; Piner, R. D.; Stankovich, S.; Jung, I.; Field, D. A.; Ventrice, C. A. Jr.; Ruoff, R. S. *Carbon* **2009**, *47*, 145.
17. Si, Y.; Samulski, E. *Nano Lett.* **2008**, *8*, 1679.
18. Muszynski, R.; Seger, B.; Kamat, P. V. *J. Phys. Chem. C* **2008**,

*112*, 5263.
19. Wang, G.; Shen, X.; Wang, B.; Yao, J.; Park, J. *Carbon* **2009**, *47*, 1359.
20. Veca, L. M.; Lu, F.; Meziani, M. J.; Cao, L.; Zhang, P.; Qi, G.; Qu, L.; Shrestha, M.; Sun, Y. P. *Chem. Comm.* **2009**, *18*, 2565.
21. Wang, G.; Yang, J.; Park, J.; Gou, X.; Wang, B.; Liu, H.; Yao, J. *J. Phys. Chem. C* **2008**, *112*, 8192.
22. Bourlinors, A. B.; Gournis, D.; Petridis, D.; Szabó, T.; Szeri, A.; Dékány, I. *Langmuir* **2003**, *19*, 6050.
23. Fan, X.; Peng, W.; Li, Y.; Li, X.; Wang, S.; Zhang, G.; Zhang, F. *Adv. Mater.* **2008**, *20*, 4490.
24. Wu, Z. S.; Ren, W.; Gao, L.; Liu, B.; Jiang, C.; Cheng, H. M. *Carbon* **2009**, *47*, 493.
25. Meng, L. Y.; Park, S. J. *J. Colloid Interface Sci.* **2010**, *342*, 559.
26. Pasricha, R.; Gupta, S.; Srivastava, A. K. *Small* **2009**, *5*, 2253.
27. Günes, F.; Han, G. H.; Kim, K. K.; Kim, E. S.; Chae, S. J.; Park, M. H.; Jeong H. K.; Lim, S. C.; Lee, Y. H. *Nano: Brief Reports and Reviews* **2009**, *4*, 83.
28. Watcharotone, S.; Dikin, D. A.; Stankovich, S.; Piner, R.; Jung, I.; Dommett, G. H. B.; Evmenenko, G.; Wu, S. E.; Chen, S. F.; Liu, C. P.; Nguyen, S. B. T.; Ruoff, R. S. *Nano Lett.* **2007**, *7*, 1888.
29. Rani, A.; Nam, S.; Oh, K. A.; Park, M. *Carbon Lett.* **2010**, *11*, 90.
30. Liu, W.; Do, I.; Fukushima, H.; Drzal, L. T. *Carbon Lett.* **2010**, *11*, 279.